Rapidity dependence of momentum anisotropies in nuclear collisions*

Ulrich Heinz[1] and Peter Kolb[2]

[1]Department of Physics
The Ohio State University
174 West 18th Avenue
Columbus, OH 43210

[2]Physik-Department
TU München
D-85747 Garching
Germany

presented at: Quark Matter 2004, Oakland, Jan. 11-18, 2004

*Work supported by the U.S. Department of Energy (DOE) and Gesellschaft für Schwerionenforschung (GSI).

Introduction: The successes of hydrodynamics at RHIC

Single particle spectra from central and peripheral Au+Au @ 130 A GeV (STAR, PHENIX):

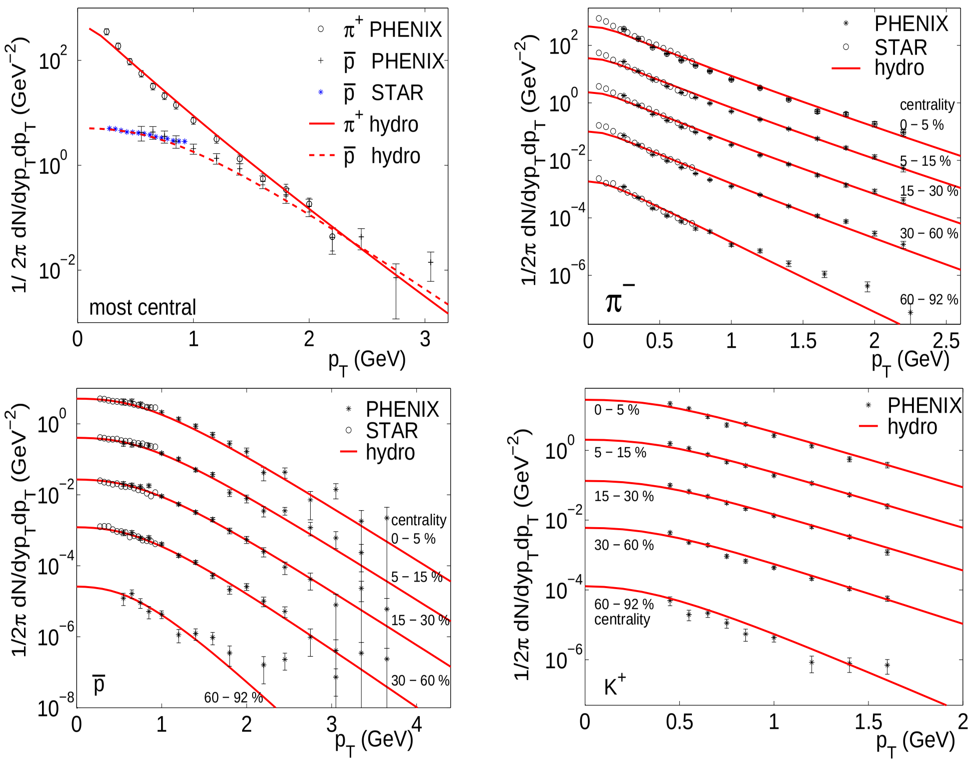

Momentum and rest mass dependence of elliptic flow (STAR, PHENIX, PHOBOS):

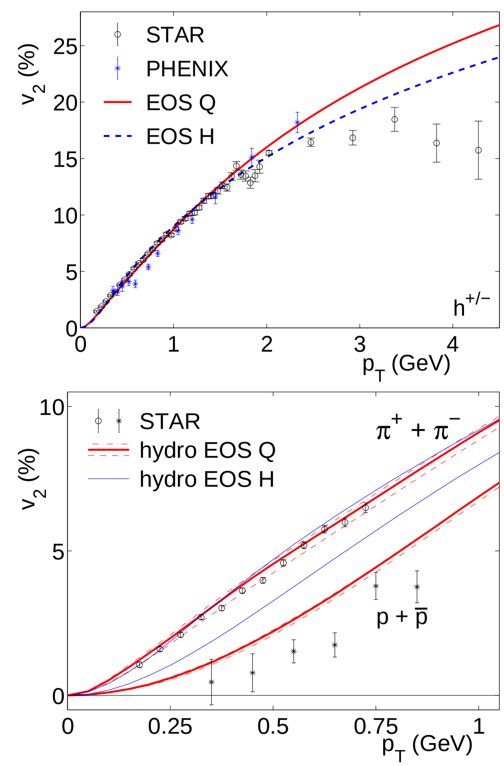

Model parameters fixed with π, $\bar{p}$ spectra at $b = 0$; all other spectra predicted (UH & PK, hep-ph/0204061).

Limits of thermalization: smaller and diluter systems

STAR, PRC 66 ('02) 034904; NA49, PRC 68 ('03) 034903

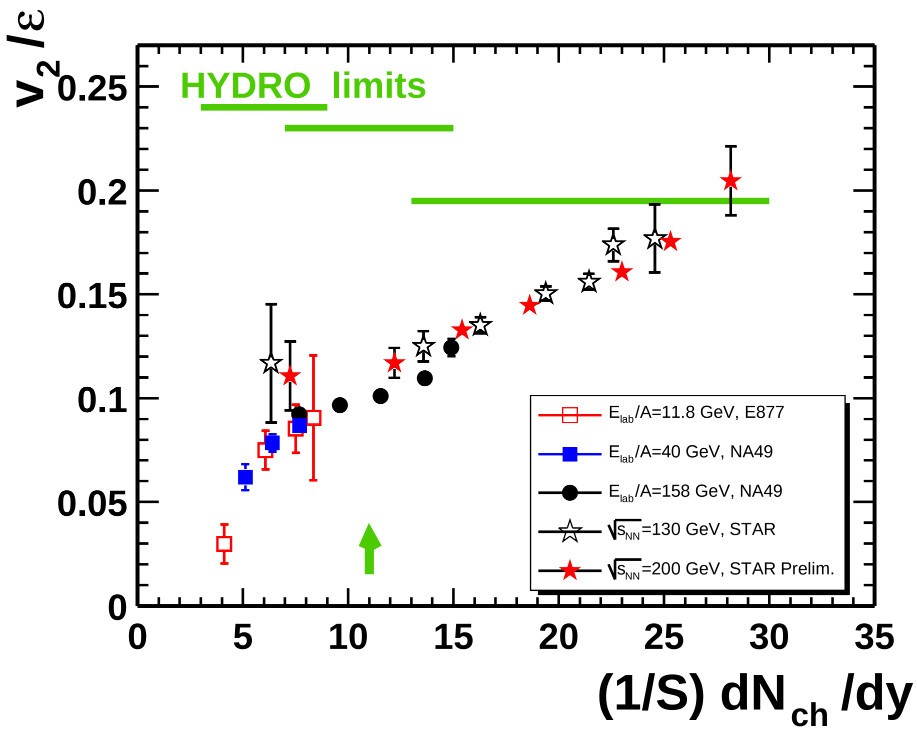

T. Hirano, PRC 65 (2002) 011901; PRC 66 (2002) 054905

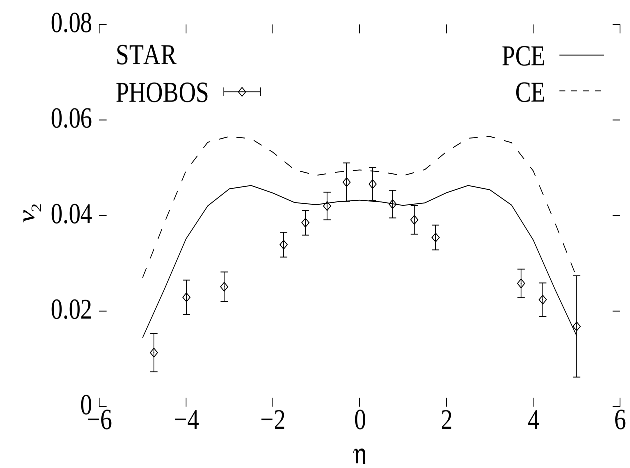

Are these two observations related?
YES!

- STAR/NA49 analysis suggests that $\frac{v_2^{\rm measured}}{v_2^{\rm hydro}}$ scales with $\frac{1}{S}\frac{dN_{\rm ch}}{dy} \propto \epsilon_{\rm Bj}(\tau{=}1\ {\rm fm}/c)$ ($S(b)$ is transverse overlap area).
- Data for scaled elliptic flow increase with initial energy density whereas hydrodynamics predicts v_2/ϵ to slightly decrease between AGS and RHIC, due to softening of EOS by quark-hadron transition (PK, Sollfrank, UH, PRC 62 (2000) 054909).

Strategy and Overview:

1. To understand rapidity dependence of elliptic flow, need model which correlates the initial transverse distribution with longitudinal position (i.e. with space-time rapidity).

2. Use weak hydrodynamic evolution in rapidity direction and Bjorken scaling $\eta_s = y$ during particle formation stage to relate initial longitudinal spatial distribution (integrated over transverse plane) with finally measured rapidity distribution in momentum space.

3. Implement momentum conservation: In non-central collisions, due to asymmetric overlap, matter at different transverse positions travels at different average rapidities $Y(x, y; b) \implies$ this correlates longitudinal and transverse coordinates in the initial entropy density profile $s(x, y, \eta_s; \tau_0)$ [Sollfrank et al. 1997, Hirano 2001].

4. From resulting initial entropy profile we compute initial energy density distribution which allows to determine the initial spatial deformation $\epsilon_x(\eta_s; b) = \langle\langle y^2 - x^2 \rangle\rangle / \langle\langle y^2 + x^2 \rangle\rangle$ as well as the transverse overlap area $S(\eta_s; b)$ as function of longitudinal position and impact parameter.

5. We use longitudinally boost-invariant hydrodynamics and the identification $\eta_s = y$ to compute from the initial $s(x, y, \eta_s; \tau_0)$ the differential directed and elliptic flows, $v_1(p_\perp, y)$ and $v_2(p_\perp, y)$, at all rapidities y for Au+Au at $b = \langle b \rangle = 6.8\,\mathrm{fm}$ (corresponding to minimum bias). All normalization constants are fixed in central collisions at $\sqrt{s} = 200\,A\,\mathrm{GeV}$.

6. The hydrodynamically calculated elliptic flow values for pions, corrected for resonance feeddown, are then multiplied with a thermalization coefficient $F_{\mathrm{therm}}(y) \leq 1$ which depends on $y = \eta_s$ through the combination $x \equiv (1/S)(dN_{\mathrm{ch}}/dy)$ and which is extracted from the NA49 compilation of the measured centrality dependence of $v_2^{\mathrm{data}}/v_2^{\mathrm{hydro}}$ at midrapidity at RHIC, SPS and AGS energies.

7. The thus corrected v_2 values are found to provide a fair representation of the PHOBOS data on $v_2(\eta)$.

8. At $\eta_s \neq 0$ the initial conditions are asymmetric with respect to the $x = 0$. This results in a nonzero differential directed flow at forward rapidities, with vanishing $p_\perp$-integral.

Mean rapidity as a function of transverse position:

Matter at transverse position (x, y) moves with average rapidity

$$Y(x,y) = \frac{1}{2}\ln\frac{dE(x,y)+dP(x,y)}{dE(x,y)-dP(x,y)} = \frac{1}{2}\ln\frac{(t_1(x,y)+t_2(x,y))+v_{\rm beam}\cdot(t_1(x,y)-t_2(x,y))}{(t_1(x,y)+t_2(x,y))-v_{\rm beam}\cdot(t_1(x,y)-t_2(x,y))}$$

where $t_{1,2} = T_A(x \pm b/2, y);\quad T_A(x,y) = \int_{-\infty}^{\infty} dz\, \rho_A(x,y,z)\,;\quad \rho_A(x,y,z) = \frac{\rho_0}{\exp((r-R_A)/a)+1}.$

Contours for $Y = 0, \pm 0.5, \pm 1, \ldots$:

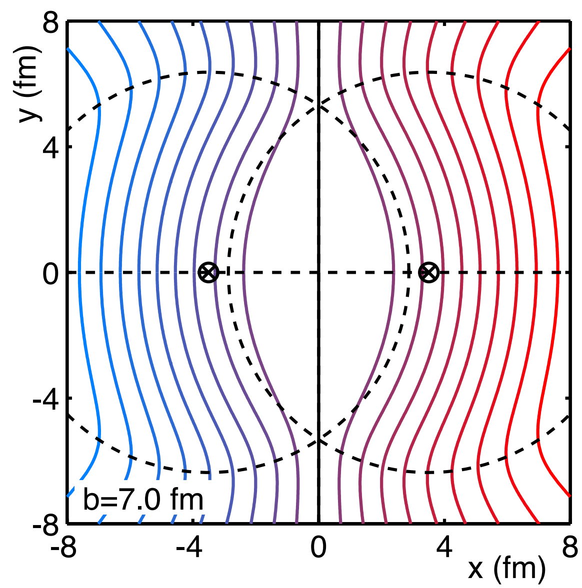

Radial increase of Y for various centralities:

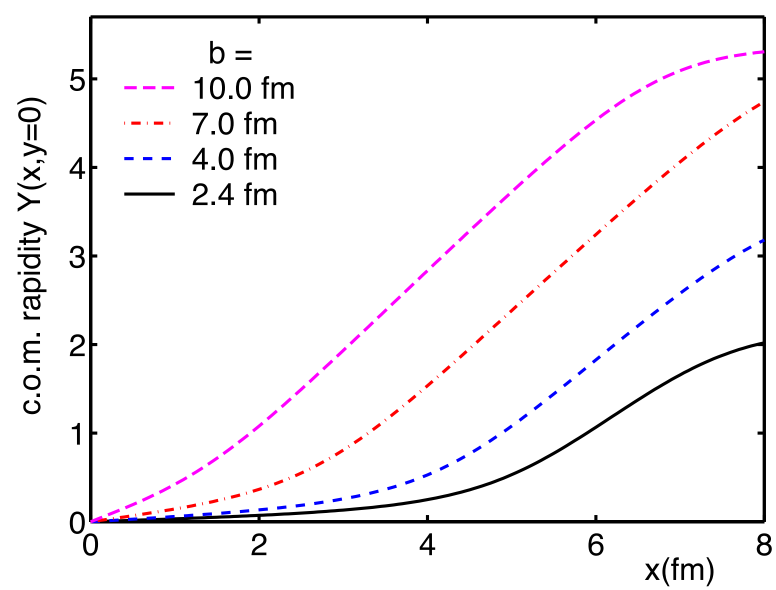

Parametrization of the rapidity spectra:

- Let initially produced quanta move on straight lines $\Rightarrow z/t = v_{\rm L} \Rightarrow \eta_s = y$.
- Hence initially $\left[\frac{dS}{dy}\right]_{\rm init} \sim \int s(\boldsymbol{r}_\perp, \eta_s{=}y; \tau_0)\, d^2r_\perp$.
- Since hydrodynamic evolution in rapidity direction is very weak (Eskola et al. (1998), Hirano et al. (2001)), we set $\left[\frac{dN_{\rm ch}}{dy}\right]_{\rm final} \propto \left[\frac{dS}{dy}\right]_{\rm init}$.
- This fixes initial longitudinal spatial distribution through measured rapidity distribution.

- The measured pseudorapidity distributions in Au+Au are well described by a double-Gaussian ansatz

$$\frac{dN_{\rm ch}}{dy} \propto e^{-\frac{(y-a)^2}{2a^2}} + e^{-\frac{(y+a)^2}{2a^2}}$$

  after transforming from y to η using $m = m_\pi$ and $\langle p_T \rangle \approx 0.4$ GeV.
- This works well for Au+Au at all centralities for $\sqrt{s} = 19.6$, 130 and 200 A GeV, using $a = 1.15$, 1.8 and 1.9, respectively (see, e.g., figure at right).
- This ansatz does *not* work for d+Au.

Au+Au @ 200 A GeV (BRAHMS PRL 88 (2002) 202301; PHOBOS PRL 91 (2003) 052303):

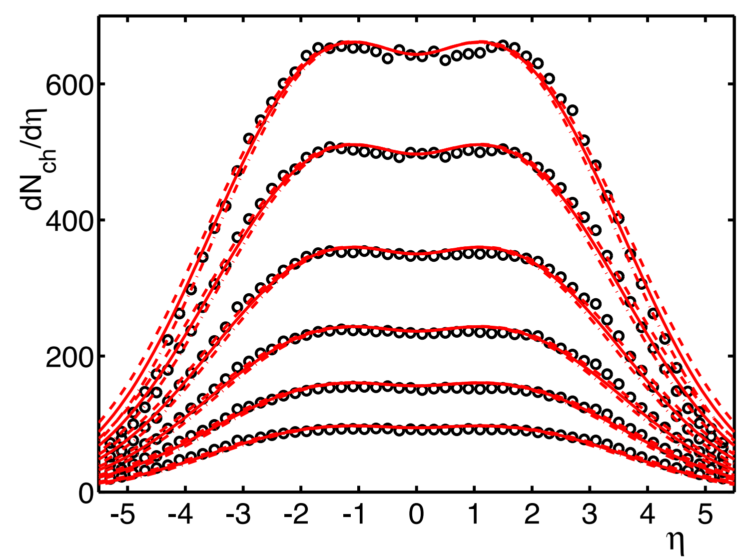

Initial 3-d density distribution

A transverse wounded nucleon density profile is distributed longitudinally by a double-Gaussian in space-time rapidity, shifted by the average rapidity $Y(x,y;b)$ of the matter at transverse position (x,y):

$$s(x,y,\eta_s;b) \propto \left(n_1^{\rm WN}(x,y;b)+n_2^{\rm WN}(x,y;b)\right)\left(e^{\frac{(\eta_S-Y(x,y;b)-a)^2}{2a^2}}+e^{\frac{(\eta_S-Y(x,y;b)+a)^2}{2a^2}}\right)$$

Contours of constant entropy density in the (x,η_s) plane

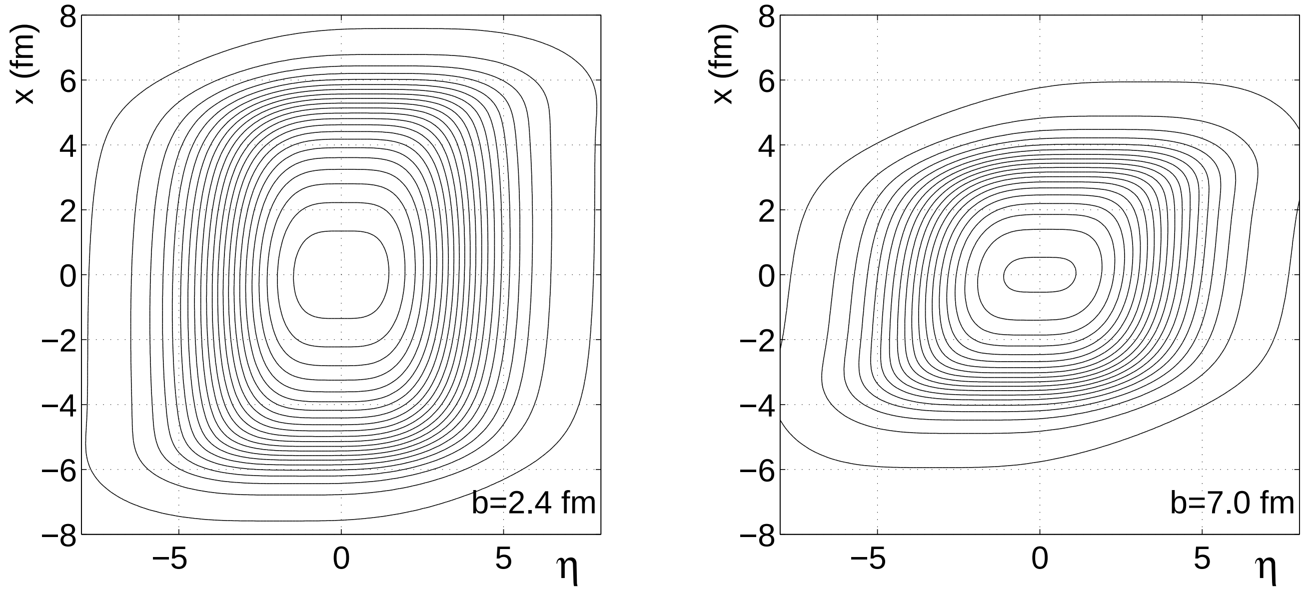

Initial transverse density distribution at non-zero rapidity

Cuts through this distribution at fixed η_s allow to determine the transverse overlap area and the transverse density distribution at different rapidities:

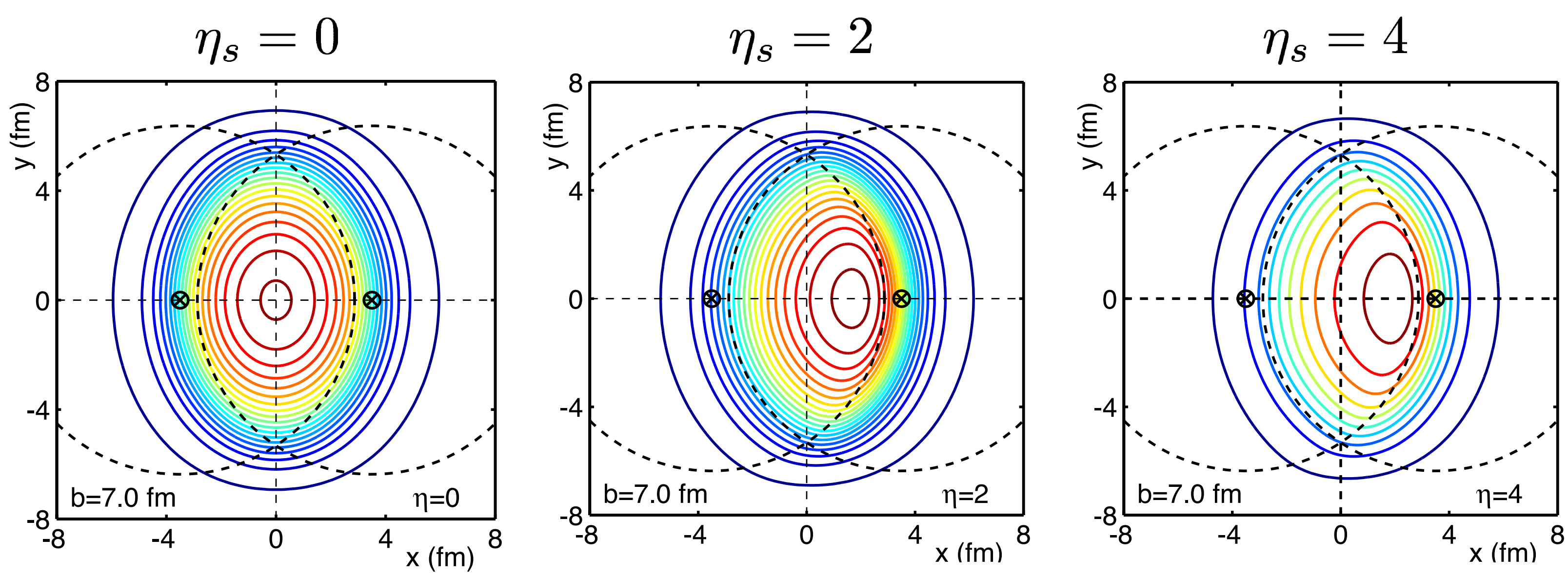

Contours of constant entropy density at different space-time rapidities

At forward rapidities, the transverse distributions become more strongly elliptically deformed ($\Rightarrow$ larger hydrodynamic v_2!) and asymmetric with respect to $x = 0$ ($\Rightarrow v_1(p_\perp) \neq 0$!).

Transverse overlap area and spatial eccentricity at $\eta_s \neq 0$

The transverse overlap area decreases at forward rapidities:

Transverse overlap area $S(\eta_s)$

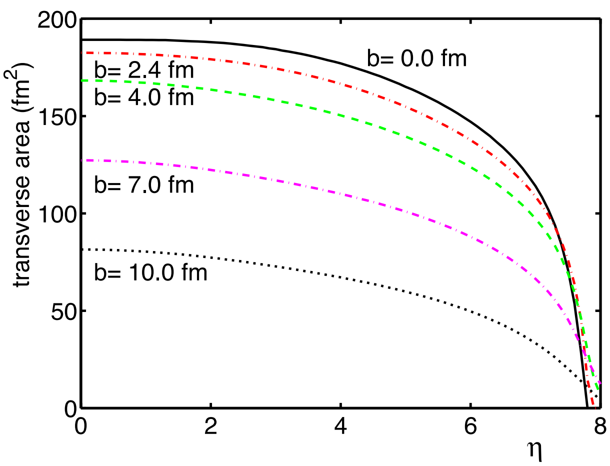

But the rapidity density dN/dy decreases faster:

$x \equiv (1/S)(dN/dy)$

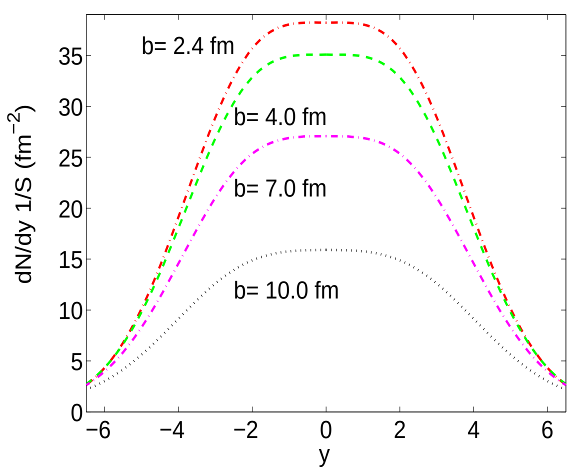

The initial spatial eccentricity increases by $\sim 15\%$ at $\eta_s > 0$:

Spatial eccentricity $\epsilon_x(\eta_s; \tau_0)$

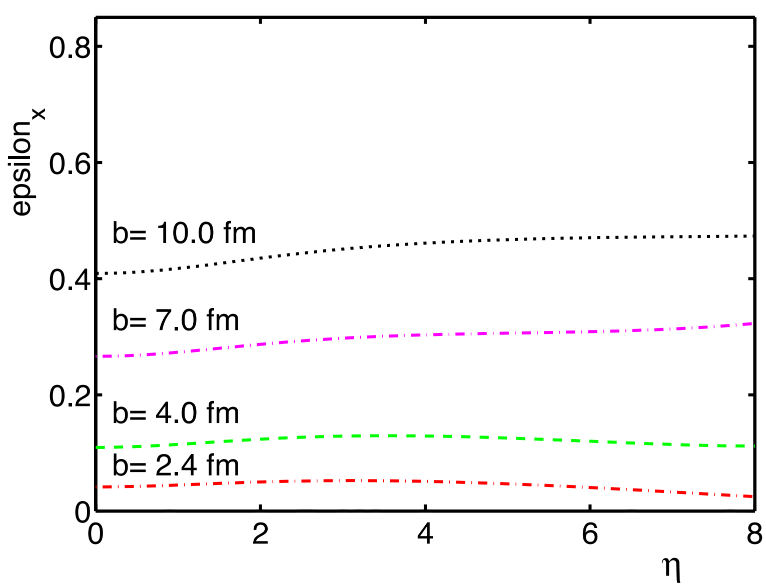

Time evolution of spatial and momentum anisotropies

Spatial eccentricity ϵ_x

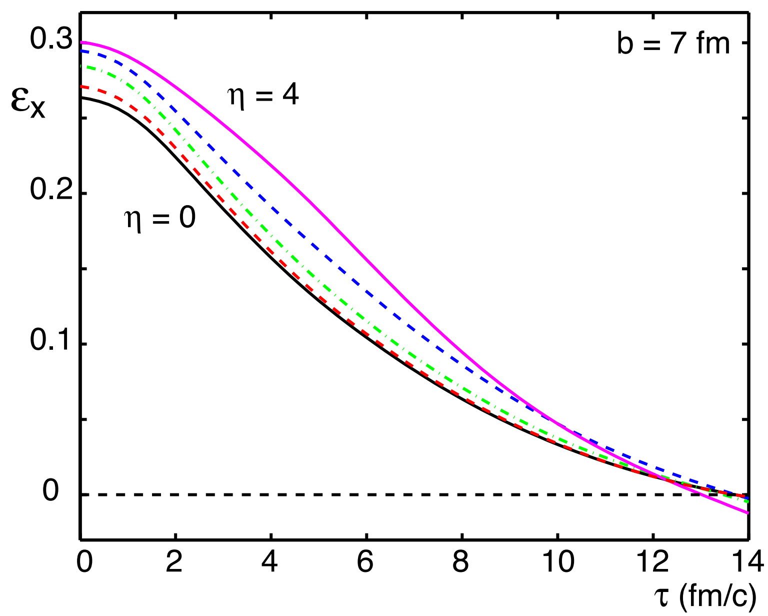

Momentum anisotropy ϵ_p

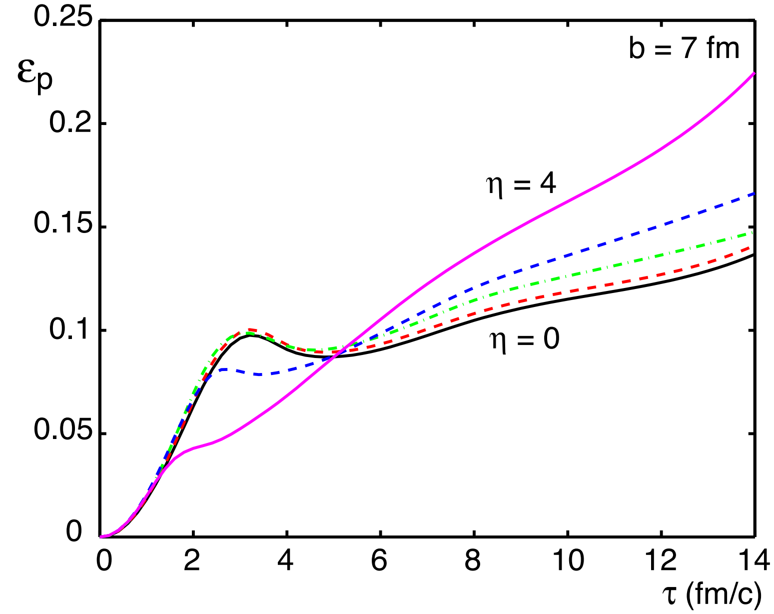

Moving towards $\eta_s > 0$ has same effect as staying at midrapidity and moving towards lower $\sqrt{s}$! (See PK, Sollfrank, UH, PRC 62 (2000) 054909)

Elliptic flow $v_2(p_\perp, y)$ at $y \neq 0$

- Elliptic flow increases at $y > 0$, due to increasing initial spatial deformation.
- Earlier freeze-out due to smaller initial energy density counteracts this at very forward rapidities.

Pions (direct pions only)

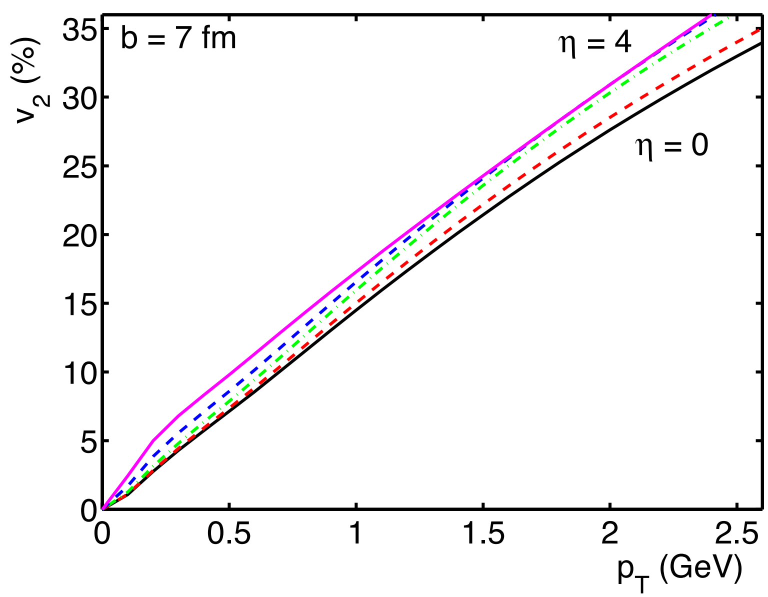

Protons (direct protons only)

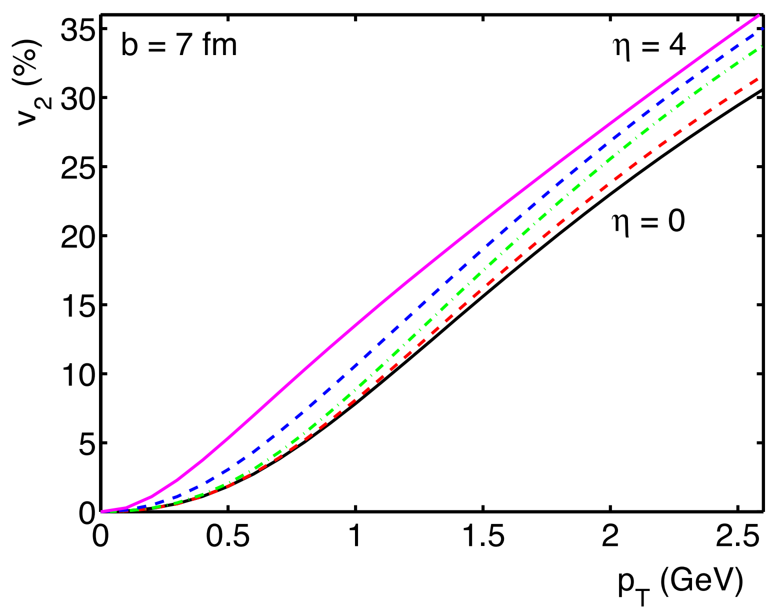

Rapidity dependence of measured elliptic flow

- The hydrodynamically calculated v_2 values for pions are reduced by hand by 15% to account for the dilution from resonance decays (see PK, Sollfrank, UH, PRC 62 (2000) 054909).
- We fit the measured ratio v_2/ϵ_x as a function of $x \equiv (1/S)(dN_{\rm ch}/dy)$ (left diagram) and reduce the hydrodynamic v_2/ϵ_x at each y by the corresponding "thermalization coefficient" $F(x)$.
- The result compares well with the PHOBOS data (right diagram).

Empirical thermalization coefficient $F(x)$

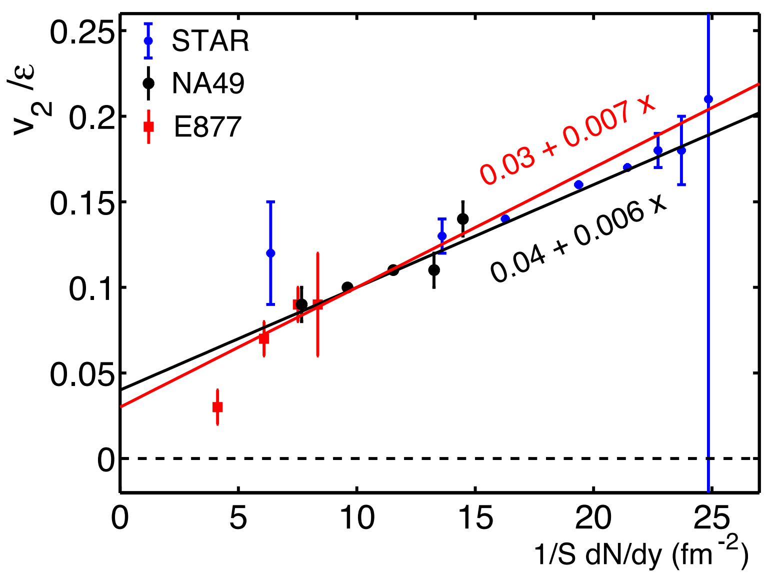

Rapidity dependence of v_2

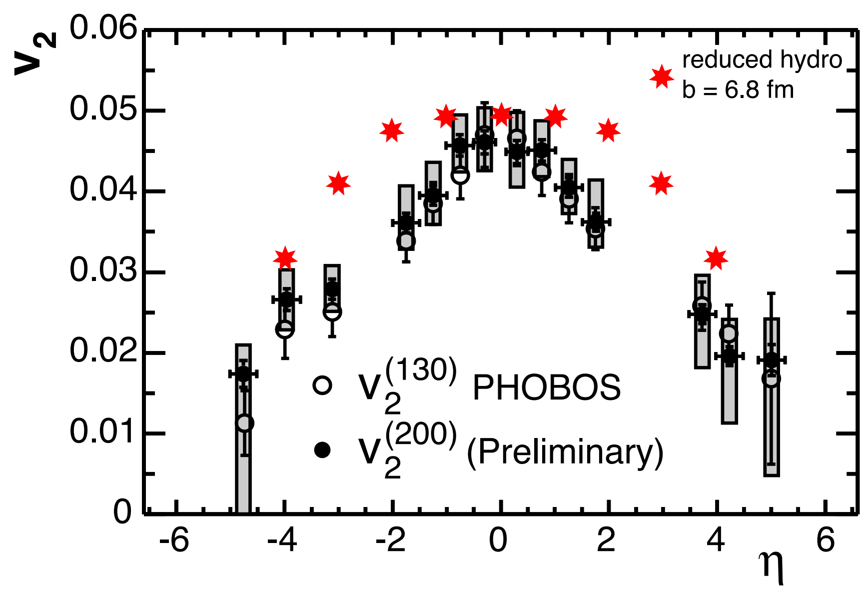

Directed flow $v_1(p_\perp, y)$ at $y \neq 0$

Although the longitudinal boost-invariance of our hydrodynamic model forbids the appearance of a non-zero v_1, the asymmetric transverse initial conditions at $\eta_s \neq 0$ cause a non-vanishing differential elliptic flow $v_1(p_\perp)$ at $y \neq 0$ whose $p_\perp$-integral with $dN/d^2p_\perp$ vanishes:

Pions (direct pions only)

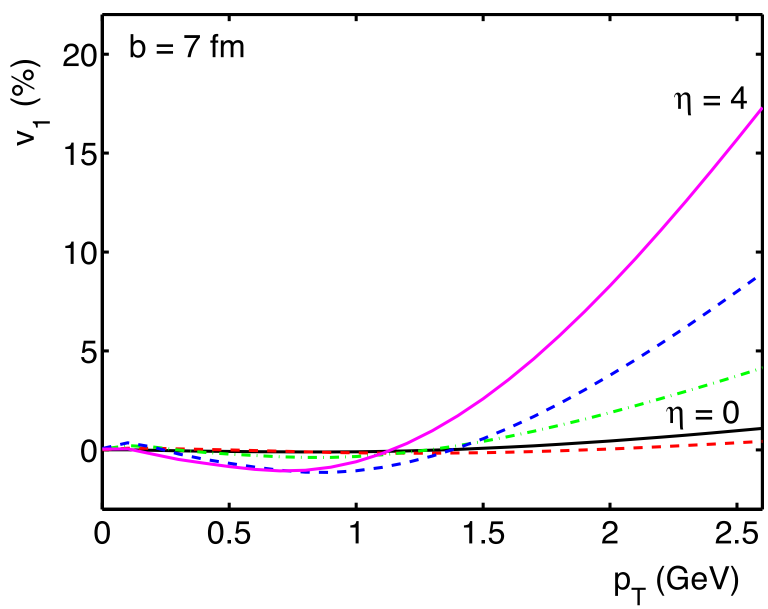

Protons (direct protons only)

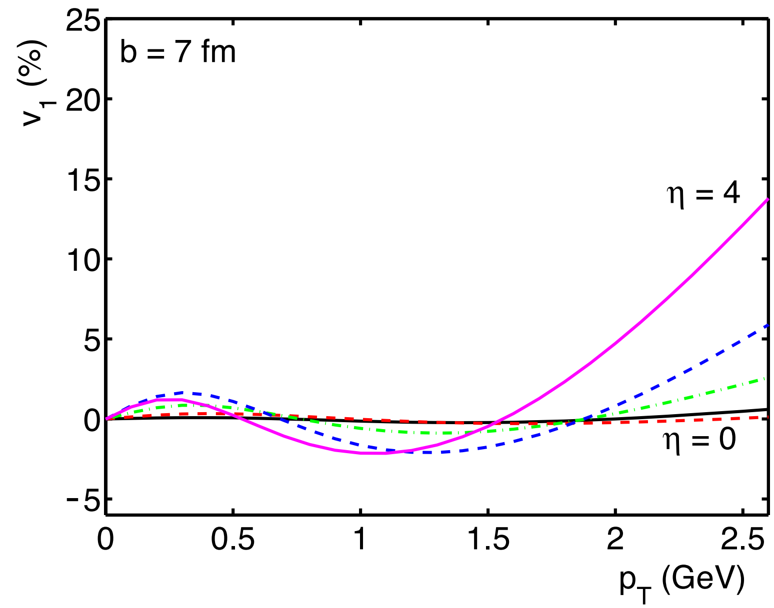

Conclusions

- The deviation from the hydrodynamic model of the observed elliptic flow in min. bias Au+Au at RHIC at forward rapidities appears to be consistent with a similar deviation at midrapidity in peripheral collisions at RHIC and for all centralities at lower collision energies.

- Whereas very good local thermal equilibrium is achieved in central Au+Au collisions at RHIC near midrapidity, thermalization gradually breaks down in smaller collision systems and at lower collision energies.

- A qualitatively consistent description of all the data is obtained by assuming that the "thermalization coefficient" F which describes the fractional degree of thermalization reached in the collision scales with the energy density at $\tau = 1\,\mathrm{fm}/c$.